

The Systemic Velocity of Eta Carinae

Nathan Smith^{*†}

Center for Astrophysics and Space Astronomy, University of Colorado, 389 UCB, Boulder, CO 80309, USA

Accepted 0000, Received 0000, in original form 0000

ABSTRACT

High-resolution spectra of molecular hydrogen in the Homunculus nebula allow for the first direct measurement of the systemic velocity of η Carinae. Near-infrared long-slit data for H_2 1-0 S(1) λ 21218 obtained with the Phoenix spectrometer on the Gemini South telescope give $V_{\text{sys}} = -8.1 \pm 1 \text{ km s}^{-1}$ (heliocentric), or $V_{\text{LSR}} = -19.7 \pm 1 \text{ km s}^{-1}$, from the average of the near and far sides of the Homunculus. This measurement considerably improves the precision for the value of $-7 \pm 10 \text{ km s}^{-1}$ inferred from neighboring O-type stars in the Carina nebula. New near-infrared spectra also provide a high-resolution line profile of [Fe II] λ 16435 emission from gas condensations known as the Weigelt objects without contamination from the central star, revealing a line shape with complex kinematic structure. Previously, uncertainty in the Weigelt knots' kinematics was dominated by the adopted systemic velocity of η Car.

Key words: circumstellar matter — stars: individual: η Car

1 INTRODUCTION

The massive star η Carinae is currently the subject of intensive spectroscopic study, especially with high-resolution techniques. An accurate and precise value for the systemic velocity is needed to interpret line profiles of the central star and to study the kinematics and geometry derived from emission lines in its circumstellar ejecta. This is especially relevant for UV echelle data with extremely high spectral resolution (e.g., Gull et al. 2004), and for any attempts to decipher orbital reflex motion if η Car is indeed an interacting binary system (Damineli et al. 2000). Yet, the radial velocity of the η Car system has been notoriously difficult to measure, because the bright central star has only broad emission lines formed in the stellar wind, and narrow emission lines arise only in spatially distinct circumstellar ejecta that are moving with respect to the star system.

Davidson et al. (1997) discussed this problem, and adopted a value for the systemic velocity of $-7 \pm 10 \text{ km s}^{-1}$ (heliocentric velocities are quoted here, unless noted explicitly). This value was inferred from an average of O-type stars in open clusters of the Carina nebula, of which η Car is a member. Davidson et al.'s adopted value deserves confirmation, though, because it is not a direct measurement of η Car itself. For most applications, typical Doppler velocities are high enough that the uncertainty of $\pm 10 \text{ km s}^{-1}$ is not a severe impediment. However, the compact ejecta near the star known as the Weigelt objects (Weigelt & Ebersberger

1986) are moving away from the star at only $\sim 50 \text{ km s}^{-1}$; for these slow condensations the $\pm 10 \text{ km s}^{-1}$ uncertainty in the systemic velocity is relatively large.

Near-infrared (IR) emission lines of molecular hydrogen arising in the polar lobes of the Homunculus (Smith 2002) provide an opportunity to measure the systemic velocity directly for the first time. Using new high-resolution data for the H_2 λ 21218 emission line, the present study confirms the accuracy of Davidson et al.'s adopted value to within about 1 km s^{-1} , and improves the precision by a factor of 10. Observations are presented in §2, the measurement of the systemic velocity is discussed in §3, and §4 presents new high-resolution measurements for the Weigelt knots and discusses corresponding implications of the systemic velocity.

2 OBSERVATIONS

High-resolution ($R \simeq 60,000$, $\sim 5 \text{ km s}^{-1}$) near-IR spectra of η Car were obtained on 2003 December 12 using the Phoenix spectrograph on the Gemini South telescope. Phoenix has a 1024×256 InSb detector with a pixel scale of $0''.085 \times 1.26 \text{ km s}^{-1}$ at a wavelength of $\sim 2 \mu\text{m}$. The $0''.34$ -wide long-slit aperture was oriented at P.A. = 310° along the polar axis of the Homunculus, and positioned on the bright central star (identical to the slit position for the central star used by Smith 2002). Sky conditions were photometric, and the average seeing was roughly $0''.5$ (although the resulting spatial resolution was better for short exposures of the central star). Sky chopping was accomplished with an observation of an off-source position roughly $35''$ to the southeast.

* Email: nathans@casa.colorado.edu

† Hubble Fellow

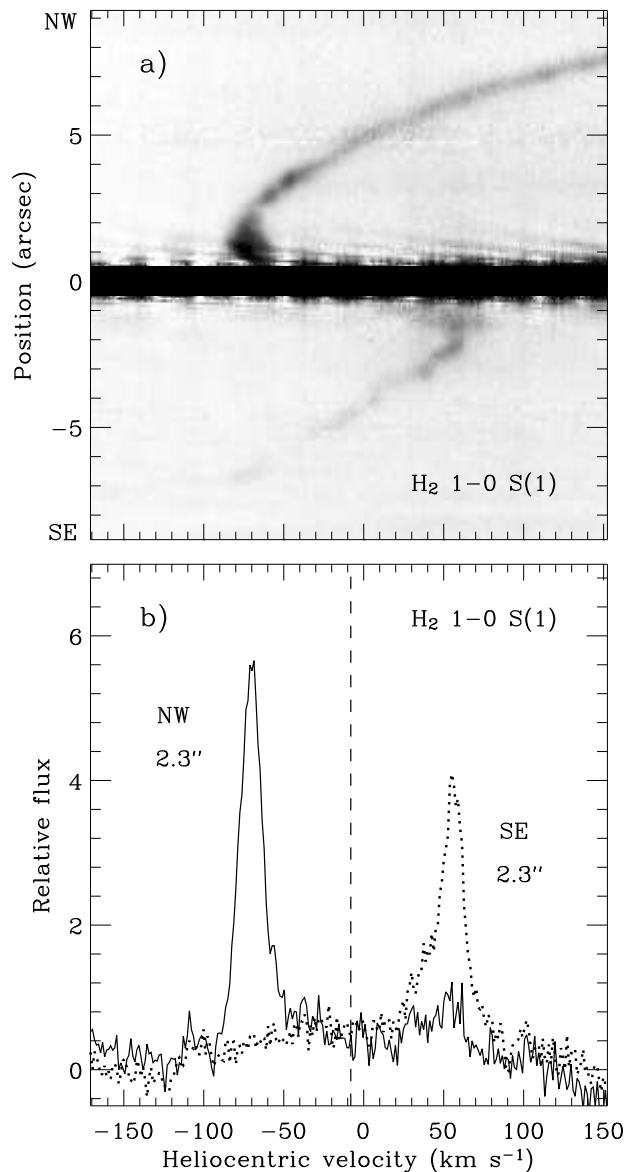


Figure 1. (a) Long-slit kinematics of molecular hydrogen emission in η Car. The thin filament extending to the northwest emits from the near side of the NW polar lobe of the Homunculus, while the fainter thin filament extending away from the star to the southeast emits from the far side of the SE polar lobe. Continuum emission has been suppressed for display here. (b) Extracted spectra from $2''.3$ on either side of the star; the northwest tracing is shown with a solid line, and the southeast tracing with a dotted line. The measured value for $V_{\text{sys}} = -8.1 \text{ km s}^{-1}$ is marked with a vertical dashed line.

A pair of 60-second exposures sampled the $v=1-0 \text{ S}(1)$ emission line of molecular hydrogen at 21218 \AA in the Homunculus, while the brightest pixels on the central star were saturated. These saturated pixels were filled-in using shorter 3-second exposures. This is only important for determining accurate positional offsets, since Smith (2002) showed that H_2 lines are absent in the spectra of the star and the Weigelt knots. Matching the wings of the point-spread function in

Table 1. H_2 Velocity Measurements

| $ R $ (arcsec) | V_{NW} (km s^{-1}) | V_{SE} (km s^{-1}) | V_{cen} (km s^{-1}) |
|-------------------|---|---|--|
| 2.0 | -72.6 | 56.0 | -8.3 |
| 2.3 | -70.3 | 53.9 | -8.2 |
| 3.1 | -53.9 | 38.3 | -7.8 |

the saturated data with those in the short exposures allowed the position of the central star to be determined to better than one pixel ($0''.085$). Figure 1(a) shows long-slit data for the H_2 line, where the reflected continuum light in the Homunculus nebula has been subtracted out. Emission from H_2 in the front side of the NW polar lobe and the far side of the SE polar lobe is apparent (see Smith 2002).

The bright standard HR 3685 was observed on the same night with the same grating settings in order to correct for telluric absorption. Numerous telluric lines were also used for wavelength calibration, using the telluric spectrum available from NOAO. Velocities were calculated adopting a vacuum rest wavelength of 21218.356 \AA for the $\text{H}_2 1-0 \text{ S}(1)$ line (Bragg, Brault, & Smith 1982), and these velocities were corrected to a heliocentric reference frame assuming an adjustment of 13.8 km s^{-1} for the motion of the Earth. (Heliocentric velocities will be quoted here; for η Car, LSR velocities are offset from heliocentric by -11.6 km s^{-1} .) Uncertainty in the resulting velocities is roughly $\pm 1 \text{ km s}^{-1}$, dominated by scatter in the dispersion solution for numerous telluric lines across the observed wavelength range.

Similar Phoenix spectra of the $[\text{Fe II}] \lambda 16435$ emission line in η Car were obtained on 2003 December 10, also on Gemini South, with the long-slit aperture having the same position angle centered on the bright star. Velocities were calculated the same way, adopting a vacuum rest wavelength of 16439.981 \AA for this line. The $[\text{Fe II}]$ line is useful with regard to some consequences of the systemic velocity for the Weigelt knots as discussed in §4. The observed $[\text{Fe II}]$ line profile is shown in Figure 2, where the integrated line flux is $5.2 \times 10^{-10} \text{ erg s}^{-1} \text{ cm}^{-2}$.

3 THE SYSTEMIC VELOCITY

Near-IR spectra with lower resolution showed that the H_2 line is emitted *exclusively* in the polar lobes (Smith 2002), so that confusing velocity components from the little homunculus (Ishibashi et al. 2003) and velocity components from the star and Weigelt knots seen in reflected light in the dusty polar lobes (Smith et al. 2003a) can be avoided. Smith et al. (2003b) also hypothesized that molecular hydrogen is coincident with a thin layer of cool dust in the outer parts of the polar lobes, which contains most of the mass in the Homunculus. This makes the 21218 \AA line an excellent tracer of the center-of-mass velocity of the Homunculus. It is a better tracer than most visual-wavelength lines; while $\text{H}\alpha$ shows a narrow peak at low heliocentric velocity (Boumis et al. 1998), it is not clear where this emission originates (Smith et al. 2000) or if it is moving with respect to the star. H_2 avoids this ambiguity. Since the Homunculus was ejected during the Great Eruption, an event which lasted about 20 years (longer than the 5.5 yr cycle of the putative

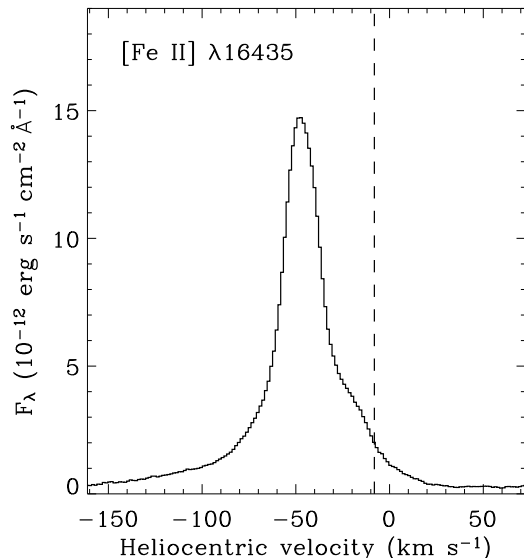


Figure 2. Continuum-subtracted [Fe II] $\lambda 16435$ emission from the Weigelt objects. This line profile was measured in a $0''.43$ -wide segment of the slit centered $0''.3$ northwest of the star. The measured value for $V_{\text{sys}} = -8.1 \text{ km s}^{-1}$ is marked with a vertical dashed line.

binary system), it seems straightforward to assume that H_2 also represents the center-of-mass of the η Car system.¹

H_2 emission from the front side of the NW polar lobe and the far side of the SE polar lobe are apparent in Figure 1. Tracings of the spectrum were made in 3-pixel ($0''.26$) wide spatial segments at three different offset positions on either side of the star at $2''.0$, $2''.3$, and $3''.1$ from the star (listed as $|R|$ in Table 1). Example tracings at $2''.3$ in each direction are shown in Figure 1(b). Velocities measured from these spectral tracings are listed in Table 1 as V_{NW} and V_{SE} . These velocity measurements in Table 1 are an average of a flux-weighted centroid and a Gaussian fit to the line profile; differences between these two measurement methods were typically $\pm 0.2 \text{ km s}^{-1}$, and in only two cases approached $\pm 1 \text{ km s}^{-1}$ when the line profiles were somewhat asymmetric, so it is a relatively unimportant source of uncertainty compared to the absolute wavelength calibration. The average of V_{NW} and V_{SE} at each position is taken as the heliocentric velocity of the center of mass of the Homunculus, V_{cen} in Table 1. The mean of the three values for V_{cen} listed in Table 1 gives -8.1 km s^{-1} for the systemic velocity of η Carinae, with an uncertainty of $\pm 1 \text{ km s}^{-1}$ due to the wavelength calibration. Correcting to the local standard of rest, the systemic velocity would be $V_{\text{LSR}} = -19.7 \pm 1 \text{ km s}^{-1}$.

¹ The only caveat here would be if the Homunculus departs from perfect axial symmetry. Morse et al. (1998) noted a slight “banana” shape to the Homunculus, which is apparent when an image of η Car is viewed upside-down. Such a departure from axial symmetry would be manifested in the data presented here as a systematic change in the centroid velocity with increasing spatial offset from the star. This is not seen within the uncertainty of the velocity measurements, so the effect is neglected here.

4 CONSEQUENCES: THE WEIGELT KNOTS

This new measurement of η Car’s systemic velocity will be useful in future studies of possible orbital reflex motion, kinematics and geometry of ejecta, or high-resolution UV echelle spectra of absorption systems, for example. The remaining discussion here is limited to immediate consequences regarding the slow-moving compact Weigelt objects. Their kinematics, including both radial velocity and proper motion measurements, have been discussed previously by several authors (Weigelt et al. 1995; Davidson et al. 1997; Dorland et al. 2004; Smith et al. 2004), and the results have been somewhat controversial. From recent proper-motion measurements using the *Hubble Space Telescope* (*HST*), Dorland et al. (2004) find an ejection date around 1934, while Smith et al. (2004) find an earlier ejection date around 1908 from similar *HST* data. For Doppler velocities, Smith et al. (2004) showed that different emission lines give different results, with velocities around -47 km s^{-1} for high-excitation UV lines, and slower speeds of roughly -40 km s^{-1} for low-excitation optical lines.

Figure 2 shows the line profile of [Fe II] $\lambda 16435$ in the Weigelt knots. This is a tracing from long-slit data where a fit to the continuum has been subtracted. The profile shows a bright narrow line core with a fainter red plateau, perhaps indicating multiple velocity components. Even the strong narrow component is resolved, with a FWHM of $\sim 22 \text{ km s}^{-1}$ compared to the spectral resolution of 5 km s^{-1} . The corresponding velocity width of about 21 km s^{-1} is too wide to be thermal broadening alone.

A flux-weighted centroid gives -46.2 km s^{-1} for the Doppler velocity of the integrated [Fe II] emission line. If instead a two-component fit is used, Doppler velocities of -46.9 and -18.1 km s^{-1} are found for the bright and faint components, respectively. These multiple velocity components or complex line shape may shed some light on different velocities for different emission lines measured by Smith et al. (2004). In particular, variable strength of the red plateau would make the average centroid velocity appear to change when observed at lower spectral resolution.

A simple interpretation like attributing the fainter component to knot B, for example, is not feasible; the red plateau has a spatial separation from the central star of $0''.27$, which is identical to that for the brighter narrow component. Interestingly, this separation is roughly consistent with the measured positions of C and/or D in *HST* images (Smith et al. 2004; Dorland et al. 2004), but not B.

Instead, a more involved explanation is likely. Suppose the emission at various Doppler velocities in Figure 2 is caused by real kinematic motion; Smith et al. (2004) proposed that slower velocities may emit from the dense neutral cores of the condensations, while faster blueshifted velocities may arise in material ablated from their outer layers. One possible interpretation for the line profile in Figure 2, then, is that the [Fe II] line is suppressed by collisional de-excitation in the slower denser cores of the Weigelt knots, while the stronger and more blueshifted emission arises in their lower-density ablated envelopes. Note that the gas which dominates the emission of [Fe II] $\lambda 16435$ is already at or above the critical density for this transition (Smith 2002). If this interpretation is correct, then the true representative velocity for the Weigelt knots would be close to -40 km s^{-1} (the

center at 1/5 of the peak emission) as suggested by Smith et al. (2004), rather than the value of -47 km s^{-1} indicated by the stronger narrow component.

Correcting these velocities for the systemic velocity, and combining them with proper motions gives clues to their three-dimensional trajectories (adopting $i=42^\circ$ as the inclination angle of the Homunculus; Smith 2002). Either of these heliocentric Doppler velocities prohibit the Weigelt knots from residing exactly in the equatorial plane of the Homunculus if they are combined with the proper motion measurements by Smith et al. (2004), given the smaller uncertainties in the new measurement of the systemic velocity presented here. Interestingly, the faster speed (-47 km s^{-1}) would place the condensations within a few degrees of the equatorial plane if the proper motions by Dorland et al. (2004) are correct. However, there is no clear reason why the Weigelt knots *must* be in the equatorial plane — as opposed to residing in the approaching polar lobe of the little homunculus, for example (the velocities measured here combined with the proper motions by Smith et al. 2004 could be consistent with this interpretation). Clearly, further study of the Weigelt knots is worthwhile. In addition to continued proper motion measurements, it would be useful to examine differences in radial velocity as a function of ionization, excitation, and especially critical density.

ACKNOWLEDGMENTS

Support was provided by NASA through grant HF-01166.01A from the Space Telescope Science Institute, which is operated by the Association of Universities for Research in Astronomy (AURA), Inc., under NASA contract NAS 5-26555. Based on observations obtained at the Gemini Observatory, which is operated by AURA, under a cooperative agreement with the NSF on behalf of the Gemini partnership: the National Science Foundation (US), the Particle Physics and Astronomy Research Council (UK), the National Research Council (Canada), CONICYT (Chile), the Australian Research Council (Australia), CNPq (Brazil), and CONICET (Argentina). These data were obtained in service observing mode, and I thank the Gemini staff, particularly Bob Blum, Ken Hinkle, and Bernadette Rodgers for their assistance.

REFERENCES

- Boumis, P., Meaburn, J., Bryce, M., & López, J.A. 1998, MNRAS, 294, 61
- Bragg, S.L., Brault, J.W., & Smith, W.H. 1982, ApJ, 263, 999
- Damineli, A., Kaufer, A., Wolf, B., Stahl, O., Lopes, D.F., & de Araújo, F.X. 2000, ApJ, 528, L101
- Davidson, K., Ebbets, D., Johansson, S., Morse, J.A., Hamann, F.W., Balick, B., Humphreys, R.M., Weigelt, G., & Frank, A. 1997, AJ, 113, 335
- Dorland, B.N., Currie, D.G., & Hajian, A.R. 2004, AJ, 127, 1052
- Gull, T.R., et al. 2004, submitted
- Ishibashi, K., et al. 2003, AJ, 125, 3222
- Morse, J.A., Davidson, K., Bally, J., Ebbets, D., Balick, B., & Frank, A. 1998, AJ, 116, 2443
- Smith, N. 2002, MNRAS, 337, 1252
- Smith, N., Davidson, K., Gull, T.R., Ishibashi, K., & Hilier, D.J. 2003a, ApJ, 586, 432
- Smith, N., Gehrz, R.D., Hinz, P.M., Hoffmann, W.F., Hora, J.L., Mamajek, E.E., & Meyer, M.R. 2003b, AJ, 125, 1458
- Smith, N., Morse, J.A., Davidson, K., & Humphreys, R.M. 2000, AJ, 120, 920
- Smith, N., et al. 2004, ApJ, 605, 405
- Weigelt, G., & Ebersberger, J. 1986, A&A, 163, L5
- Weigelt, G., et al. 1995, RevMexAA Ser. Conf., 2, 11